Indian Journal of Engineering & Materials Sciences
Vol. 32, August 2025, pp. 502-508
DOI: 10.56042/ijems.v32i04.21052

Analysis of motor-battery combinations in EV system

Pravallika Gandhaveeti*& P. Sujatha
Department of EEE, JNTUA College of Engineering, Anantapur 515 001, Andhra Pradesh, India

Received: 27 June 2025; accepted: 29 July 2025

Electric vehicles (EVs) have appeared as a potential option, giving zero emissions and a cleaner means of transportation. However, as the adoption of EVs has increased, the selection of the right motor and battery combination has become ever more important. This study has examined the performance of Brushless DC (BLDC), Induction Motor (IM), and Permanent Magnet Synchronous Motor (PMSM) for electric vehicle traction applications when powered by lithium-ion batteries. Because of its precision, quick dynamic response, and simplicity in attaining appropriate speed and torque control, the Field-Oriented Control (FOC) technique with PI controller has been used in this work. The simulation model and results have been carried out and compared by using MATLAB Software.

Keywords: Brushless DC motor (BLDC), Electric vehicles (EVs), Field-oriented control (FOC), Induction motor (IM), MATLAB software, Permanent magnet synchronous motor (PMSM)

1 Introduction

Electric vehicles (EVs) are developing as an evolutionary force in the automotive industry, giving a range of environmental and economic benefits. Their primary advantage lies in reducing urban pollution, as they produce zero emissions, unlike conventional internal combustion engine (ICE) automobiles, which create greenhouse gasses and hazardous pollutants[1]. One of the most compelling aspects of electric vehicles is their cost-effectiveness. In comparison to gasoline or diesel-powered vehicles, EVs boast lower running costs. This is largely because electricity, especially when generated from renewable sources, is cheaper and more stable in price than fossil fuels. Moreover, EVs have less moving parts, resulting in lower maintenance expenses[2]. The major requirements for the consumers in EV industries are the mileage, speed, performance, efficiency, high storage battery and its protection and cost of EV[3]. Electric motors and battery technology play important roles in determining the range and performance of electric vehicles. The most popular motors utilised in electric vehicles (EVs) are DC and AC motors. AC motor drives provide several notable benefits over their DC equivalents, including higher power density, higher efficiency, robustness, effective regenerative braking, reduced maintenance requirements and reliability[4-5]. Induction Motors, BLDC Motors, and PMSM Motors are the most common types of EV traction AC motors. However, a comparative investigation of these motors is complex but remains a challenge[6]. The two most prominent vector control systems are Field-Oriented Control (FOC) and Direct Torque Control (DTC). Despite its simple construction, DTC has excellent dynamic behaviour; yet, it has a higher torque ripple[7]. In comparison to DTC, FOC has a better dynamic response and less torque ripple[8-12]. In electric vehicles (EVs), batteries act as the primary energy source, and their choice plays a vital role in defining the vehicle's range, overall efficiency, performance, and cost. Several categories of batteries have been used in EV applications, each with distinct characteristics, advantages, and limitations[13]. The most prevalent battery kinds are lead acid, nickel-based, and lithium-ion. Among them, lithium-ion batteries are broadly accepted owing to their high energy density, extended lifespan, and high efficiency[14-15]. In this article, the performance of Brushless DC motor, Induction Motor and Permanent Magnet Synchronous Motor for use in electric vehicles is studied using MATLAB software in terms of speed/accelerating characteristics, rotor speed, and state of discharge characteristics.

The subsequent sections of this study are outlined below. Section 2 discusses several driving models and their control and also introduces the electric vehicle configuration. Section 3 discuses and compares the simulation findings and Section 4 introduces the conclusion.

*Corresponding author (Email: pravallikagandhaveeti@gmail.com)

2 Materials and Methods

2.1 Mathematical modelling of induction motor

In Fig. 1, the 1-φ Circuit model of a 3-φ induction motor is illustrated. In this representation, $\vec{V}_s$ denotes the voltage vector of stator, and $\vec{I}_s$ represents the current vector of stator. The parameter r_s and r_r are the stator and rotor equivalent resistance referred to the stator side. L_{ls} and L_{lr} are the stator and rotor leakage inductances respectively, also mentioned to the stator side. L_m indicates inductance due to magnetization, and L_s represents the self-inductance. The slip is denoted by s. Using Field-Oriented Control (FOC), The dq-axis stator voltage components enable separate control of both flux and torque in the motor. The dq reference frame aligns with the flux vector of rotor, rotating synchronously at ω_e. The induction motor's dynamic equation of stator voltage in this synchronous frame is:

$$v_{ds} = (r_s + p\sigma L_s)i_{ds} + \frac{L_m}{L_r}p\lambda_{dr} - \omega_e[\frac{L_m}{L_r}\lambda_{qr} + L_s\sigma i_{qs}] \quad \ldots (1)$$

$$v_{qs} = (r_s + p\sigma L_s)i_{qs} + \frac{L_m}{L_r}p\lambda_{qr} + \omega_e[\frac{L_m}{L_r}\lambda_{dr} + L_s\sigma i_{ds}] \quad \ldots (2)$$

Orienting the rotor flux vector along the direct axis can result in the FOC. i.e. $\lambda_{qr} = 0$ and $p\lambda_{qr} = 0$. Then,

$$\begin{bmatrix} v_{ds} \\ v_{qs} \end{bmatrix} = \begin{bmatrix} r_s + p\sigma L_s & -\omega_e\sigma L_s \\ \omega_e\sigma L_s & r_s + p\sigma L_s \end{bmatrix}\begin{bmatrix} i_{ds} \\ i_{qs} \end{bmatrix} + \frac{L_m}{L_r}p\lambda_{dr}\begin{bmatrix} 1 \\ \omega_e \end{bmatrix} \quad \ldots (3)$$

The electromagnetic torque can be stated as,

$$T_e = \frac{3}{2} \times \frac{P}{2} \times \frac{L_m}{L_r}\lambda_{dr} i_{qs} \quad \ldots (4)$$

Here, v_{ds} and v_{qs} represent the d-axis and q-axis stator voltages, λ_{dr} and λ_{qr} represents the rotor's d- and q-axis flux linkage and leakage factor, P represents the No of poles, and p=d/dt.

2.2 Mathematical modelling of BLDC motor

In Fig. 2, the 1-φ circuit model of a 3-φ brushless DC (BLDC) motor is depicted. In this circuit, $\vec{V}_s$ represents the voltage vector of stator, while $\vec{I}_s$ denotes the current vector of stator. The parameter r_s corresponds to the equivalent resistance of stator, L_{ls} is the leakage inductance of stator winding, L_s represents the self-inductance, and E_{BLDC} is the back electromotive force (EMF) generated by the PM. Using the Field-Oriented Control (FOC) strategy to achieve decoupled torque control, the 3-φ oscillatory stator currents are converted to a Orthogonal rotating reference frame (d-q axes), where they appear as DC values. The reference frame maintains alignment with the field vector of rotor, synchronously rotating at angular velocity ω_r. The BLDC motor's dynamic stator voltage equation in this synchronous rotating frame is given by:

$$\begin{bmatrix} v_{ds} \\ v_{qs} \end{bmatrix} = \begin{bmatrix} r_s + pL_s & -\omega_r L_s \\ \omega_r L_s & r_s + pL_s \end{bmatrix}\begin{bmatrix} i_{ds} \\ i_{qs} \end{bmatrix} + P_t(\theta_r)\begin{bmatrix} e_a \\ e_b \\ e_c \end{bmatrix} \quad \ldots (5)$$

Where, e_a, e_b and e_c are stator back EMF, stated as,

$$\begin{bmatrix} e_a \\ e_b \\ e_c \end{bmatrix} = p\begin{bmatrix} \psi_{ra} \\ \psi_{rb} \\ \psi_{rc} \end{bmatrix} = \omega_r K_e \begin{bmatrix} f_{as}(\theta_r) \\ f_{bs}(\theta_r) \\ f_{cs}(\theta_r) \end{bmatrix} \quad \ldots (6)$$

Equation (5) can be rewritten as,

$$\begin{bmatrix} v_{ds} \\ v_{qs} \end{bmatrix} = \begin{bmatrix} r_s + pL_s & -\omega_r L_s \\ \omega_r L_s & r_s + pL_s \end{bmatrix}\begin{bmatrix} i_{ds} \\ i_{qs} \end{bmatrix} + \omega_r K_e \begin{bmatrix} f_d(\theta_r) \\ f_q(\theta_r) \end{bmatrix} \quad \ldots (7)$$

In the *dq* reference frame, the torque stated as follows.

$$T_e = \frac{3}{2} \times \frac{P}{2} \times [K_e f_q(\theta_r) i_{qs} + K_e f_d(\theta_r) i_{ds}] \quad \ldots (8)$$

The stator voltages on the d and q axes are represented by v_{ds} *and* v_{qs}, respectively. ψ_{ra}, ψ_{rb},

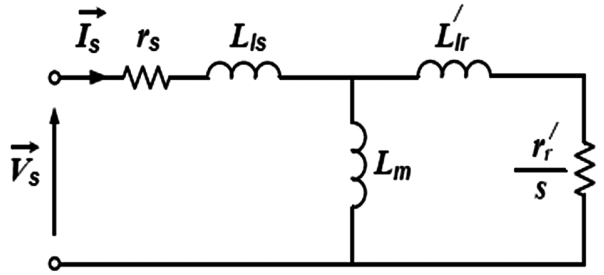

Fig. 1 — Single-phase equivalent representation of the 3-φ induction motor circuit.

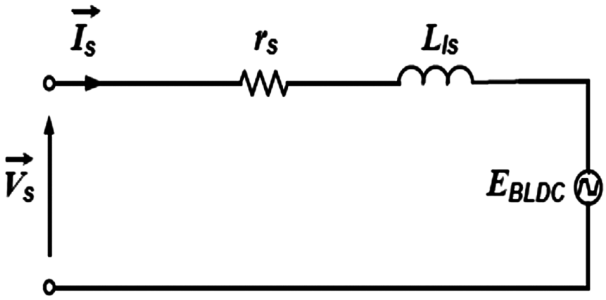

Fig. 2 — Single-phase equivalent representation of the 3-φ BLDC motor circuit.

ψ_{rc} are fluxes between rotor magnets and stator coils, $K_e$is the back-EMF coefficient, θ_r is the angular position of rotor, and $f_{as}(\theta_r), f_{bs}(\theta_r), f_{cs}(\theta_r)$ are the regularized back-EMF functions. P represents the No of poles, i_{ds}, i_{qs} are the stator currents of d- and q-axis respectively, P_t duplicates the park transform, and $p = \frac{d}{dt}$.

2.3 Mathematical modelling of PMSM motor

In Fig. 3, the 1-φ circuit model of a 3-φ PMSM is depicted. Here, $\vec{V_s}$ represents the voltage vector of stator, $\vec{I_s}$ is the current vector of stator, r_s denotes the equivalent resistance of stator, L_{ls} is the leakage inductance of stator, L_s represents the intrinsic inductance, and E_{PMSM} is the EMF generated by the PM. Applying Field-Oriented Control (FOC) to attain decoupled torque control, Thevoltage components of stator in dq coordinates are regulated within a reference frame that tracks the ω_r-speed rotation of the rotor field. The quadrature-axis rotor flux is zero because the rotor flux is aligned along the d-axis and there is no flux in the q-axis. The governing dynamic equations for PMSM stator operation are given below:

$$\begin{bmatrix} v_{ds} \\ v_{qs} \end{bmatrix} = \begin{bmatrix} r_s + pL_s & -\omega_r L_s \\ \omega_r L_s & r_s + pL_s \end{bmatrix} \begin{bmatrix} i_{ds} \\ i_{qs} \end{bmatrix} + \begin{bmatrix} W_r \psi_f \\ p\psi_f \end{bmatrix} \quad \ldots (9)$$

The d and q-axis components of the stator flux are defined as follows:

$$\psi_{ds} = L_s i_{ds} + \psi_f \quad \ldots (10)$$

$$\psi_{qs} = L_s i_{qs} \quad \ldots (11)$$

In the dq frame, the torque stated as follows:

$$T_e = \frac{3}{2} \times \frac{P}{2} \times [\psi_{ds} i_{qs} - \psi_{qs} i_{ds}] \quad \ldots (12)$$

In this the dq-axis stator voltages are denoted by v_{ds} and v_{qs}respectively, while the d and q-axis stator flux linkages are represented by ψ_{ds} and ψ_{qs}respectively, and the rotor PM flux linkage is represented by ψ_f.The d-axis and q-axis stator currents are represented by i_{ds}, i_{qs}, the number of poles denoted by p and $p = \frac{d}{dt}$.

2.4 Battery modelling

The second-order ECM model's single-cell Li-ion battery is composed of two parallel RC circuits connected in series. This model reflects the battery's dynamic and stable state with an ohmic resistance of R_s. It has a V_{oc}, which stands for open-circuit voltage source. The terminal voltage is V_t, while the charging and discharging current is I(t). Fig. 4 depicts the comparable circuit model for a second-order lithium-ion battery.

The Lithium-Nickel-Manganese-Cobalt-Oxide (LiNiMnCoO2) cell, is the battery used in this work to power the IM and BLDC drives. It features a 3.7-volts operating voltage and a nominal capacity of 2000mAh.

2.5 Electric vehicle configuration

The following discussion elaborates on the complete configuration and operational control schematic of an EV as shown in Fig. 5 and the power flow illustration of EV is as shown in Fig. 6a. Here, the rear axle is driven by the IM/BLDC/PMSM via the differential and transmission. A Lithium-Ion battery is utilized to store energy and give the necessary power to the motor via a universal bridge. The appropriate 3- phase AC voltage is provided to the motor stator via a converter, and the converter output is regulated by an appropriate gate signal from the motor controller. Here the torque sensor feedback is critical for adjusting the motor's operation, ensuring that the torque delivered to the rear axle wheels matches the required performance. The cruise controller compares the reference speed from the

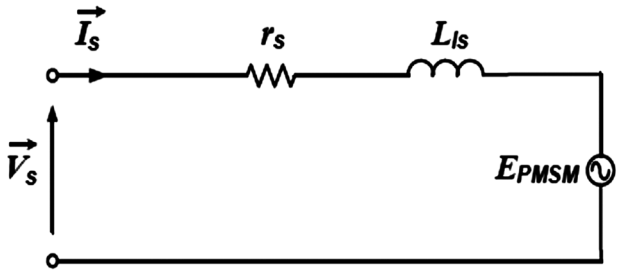

Fig. 3 — 1-φ equivalent representation of the 3-φ PMSM motor circuit.

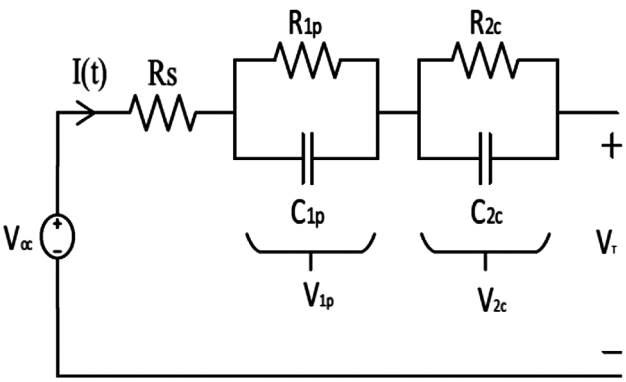

Fig. 4 — Second order electric circuit model.

FTP75 drive cycle as shown in Fig. 6b with the actual speed and adjusts the motor torque accordingly, ensuring optimal energy consumption and smooth driving experience. To achieve decoupled torque-speed control, a FOC with PI controller is employed. The PI controller is employed to regulate the motor's current and/or speed to achieve precise control and stability. The control law employed in this method is given by,

$$T = K_p e + K_i \int e \; dt \quad \ldots (13)$$

Its output involves updating the PI controller gains (K_p and K_i) according to a set of rules, ensuring optimal control performance even in the face of parameter variations and drive nonlinearity. and the following K_p *and* K_i values are listed in table 1. Here, 3-φ pulsating quantities are transformed into 2-φ DC

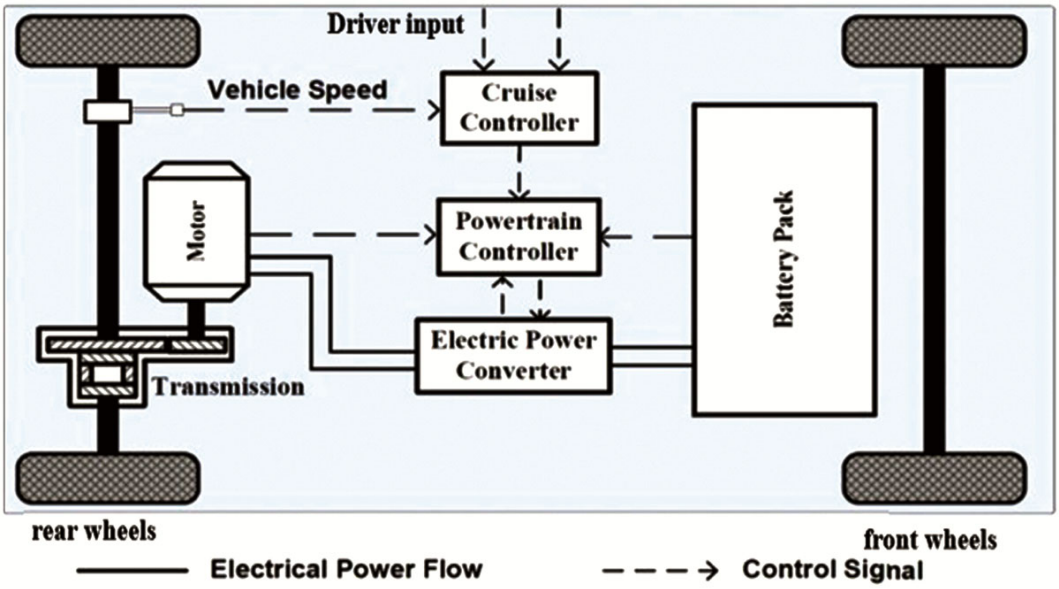

Fig. 5 — Schematic representation of electric vehicle with AC motor-based traction system.

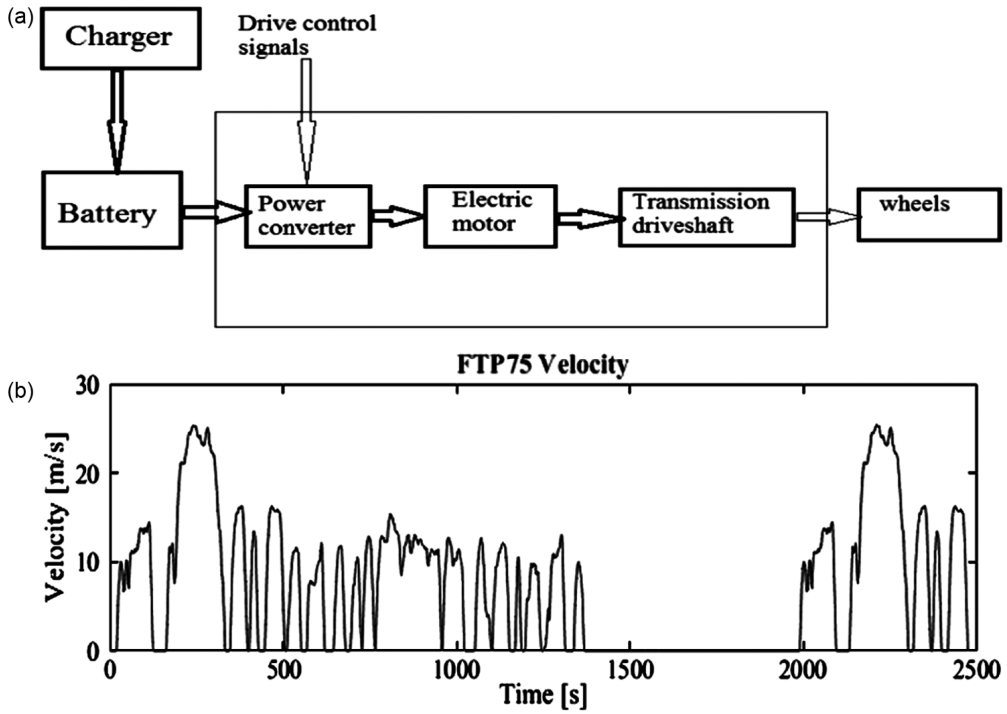

Fig. 6 — (a) Power flow diagram of EV and (b) Drive cycle source used in simulation.

quantties in the d-q time-invariant domain, with appropriate alignment to enable faster and more effective control.

3 Results and Discussion

An analytical comparison of an Induction Motor-based EV and a BLDC motor-based EV and PMSM based EV is performed using MATLAB/Simulink, with simulations based on the FTP75 drive cycle. The comparison evaluates vehicle velocity/speed, rotor speed, electromagnetic torque, battery state of charge (SoC), battery voltage, and current. Details of the different motors and Lithium-ion battery parameters can be found in Table 1 and 2. The FTP75 drive cycle source is used as a reference speed to examine the performance of EVs. First, the results for the IM drive are presented, followed by the test results for the BLDC and PMSM drive. Figures. 7(a-c) show the simulation results of vehicle speed when an BLDC, IM and PMSM motor are connected. Where it is detected that, in case of the IM and PMSM, the vehicle speed increases with respect to the reference and works effectively at higher speeds. For the BLDC motor, the vehicle speed increases with the reference speed at starting, but at high speeds, the BLDC motor may not perform as effectively as compared to other motors. Table 3 illustrates the comparison of speed test results of the IM, BLDC and PMSM motors. The simulation results of rotor speed of IM, BLDC and PMSM motors are shown in Figs. 8(a-c). Here, the PMSM runs at a higher speed compared to the BLDC and IM motor. Figures 9(a-c) show the electromagnetic torque response of particular motors. All motors experience electromagnetic torque variations as their speeds change and following their respective load torque perfectly. However, PMSM motors have showed high starting torque compared to IM and BLDC motors, as it enhances the acceleration, load capacity and driving experience without need of complex transmission. Figures (10-12) show the current and voltage drawn from the battery for each of the three drives and the changes in battery SoC (charging/discharging) during individual drive operations are analysed. It is observed that the PMSM motor demonstrates the most efficient performance.

Table 1 — Motor parameters used in EV.

Parameters IM		BLDC Motor	PMSM Motor
Rated power	15kW	15kW	15Kw
Rated speed	1460rpm	3000rpm	3000rpm
Inertia	0.05	0.0027	0.0027
No of poles	4	8	8
Proportional gain (k_p)	1	100	1
Integral gain (K_i)	1	0	1

Table 2 — Lithium-ion battery parameters.

Nominal value	400V
Initial State of Charge (SOC)%	95
Rated Capacity	100Ah
Battery Response Time	30s
Cut-off Voltage	300V
Fully charged voltage	465.5949V
Maximum capacity	100Ah
Nominal discharge current	43.4783A
Internal resistance	0.04 Ω
Capacity at nominal voltage	90.4348 Ah

Table 3 — Comparison of vehicle speed test results for induction, BLDC and PMSM motors.

Speed test time(sec)	Drive cycle source as a reference (m/s)	Induction motor (m/s)	BLDC motor (m/s)	PMSM motor (m/s)
20-40 sec	7.22	6.8	6.09	6.914
40-60 sec	8.595	8.851	9.19	8.976
60-80 sec	11.2	10.88	11.32	10.93
80-100 sec	13.3	13.2	11.98	13.22

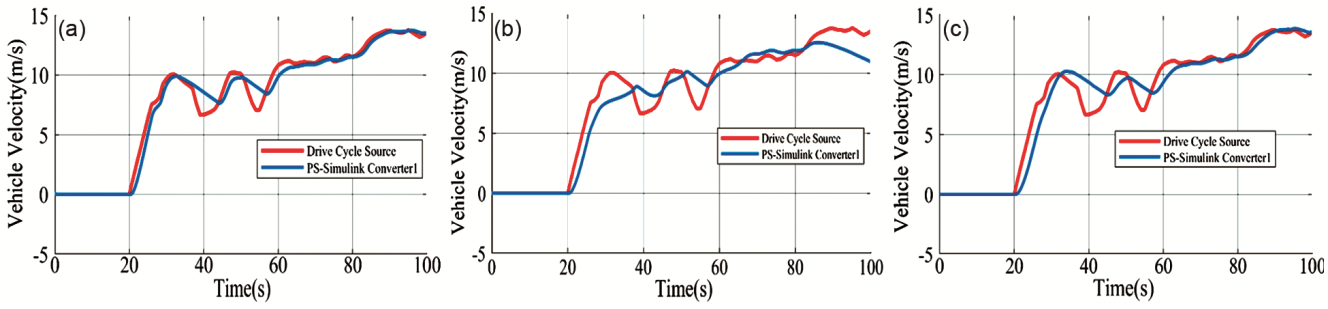

Fig. 7 — Graphs of vehicle velocity while using (a) IM, (b) BLDC, and (c) PMSM motor.

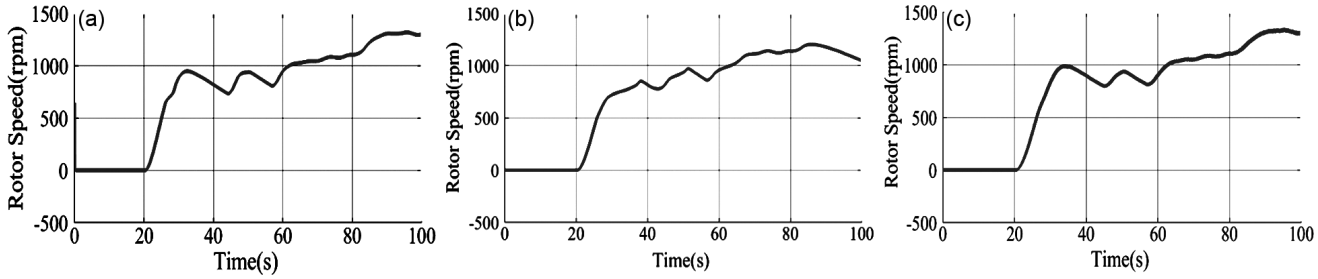

Fig. 8 — Graphs of rotor speed of (a) IM, (b) BLDC, and (c) PMSM motor.

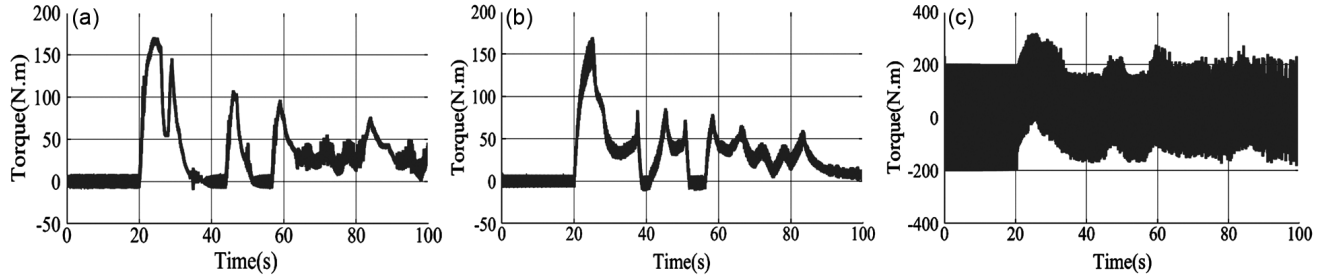

Fig. 9 — Graphs of electromagnetic torque while using (a) IM, (b) BLDC, and (c) PMSM motor.

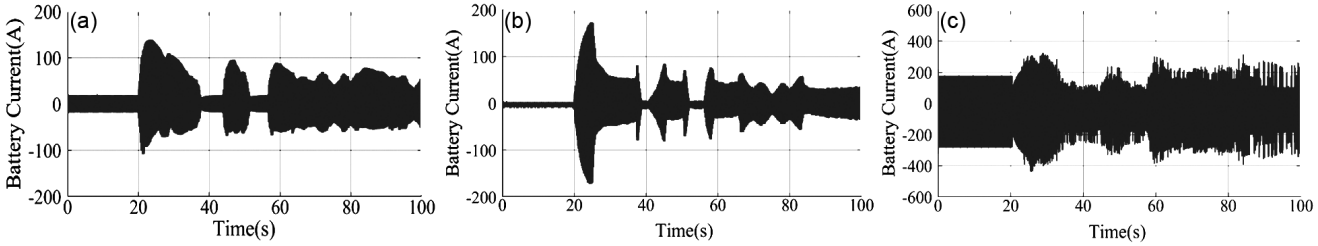

Fig. 10 — Graphs of battery current when operating with (a) IM, (b) BLDC, and (c) PMSM motor.

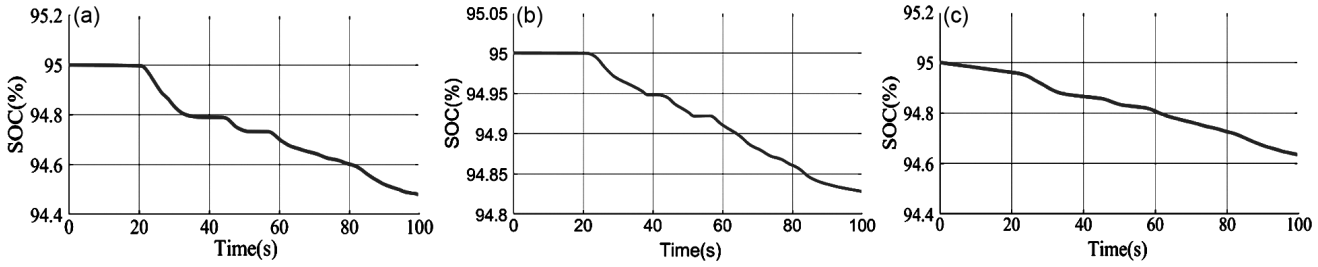

Fig. 11 — Graphs of battery SOC when operating with (a) IM, (b) BLDC, and (c) PMSM motor.

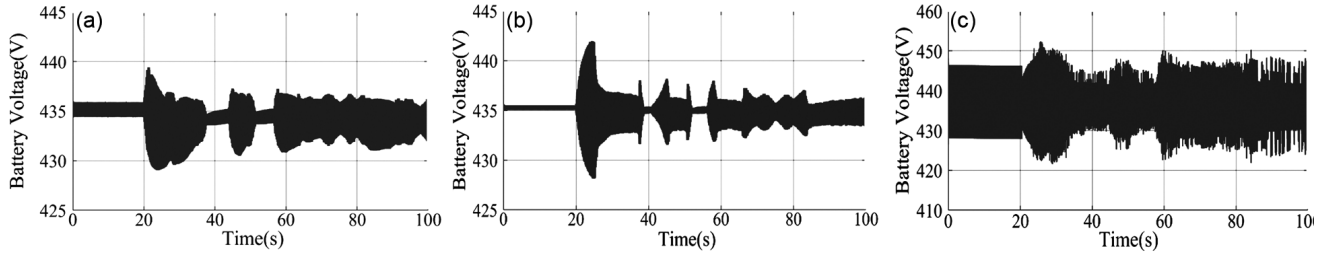

Fig. 12 — Graphs of battery voltage while using (a) IM, (b) BLDC, and (c) PMSM motor.

4 Conclusion

This paper evaluates the performance of Brushless DC (BLDC) motors, Induction Motors (IM), and Permanent Magnet Synchronous Motors (PMSM) for electric vehicle traction applications when powered by lithium-ion batteries are investigated by using MATLAB Software. From this it can be concluded that while BLDC motors are effective at lower to mid-range speeds, IM and PMSM Motors outperform them at higher speeds, making IM and PMSM more suitable for applications requiring sustained high-speed operation. The rotor speed also reflects this, with PMSMs able to maintain a higher rotational speed than IM and BLDC motors. Among all motors the PMSM motor more suitable for electric vehicles where battery efficiency and range are critical factors, as it can deliver strong performance while using less battery power, allowing for longer driving ranges and more efficient energy consumption.

Conflict of Interest

On behalf of all authors, the correspond ding author states that there is no conflict of interest.

References

1 Julio A, Sanguesa, Vicente Torres-Sanz, Francisco, Martinez J & Marquez-Barja. M, *Smart Cities*, 4(2021)372.

2 Kavuri, Kuzhivila P N & Sireesha. K, *A Comparative study on Electric Vehicle and Internal Combustion Engine Vehicles*, Proceedings of the International Conference on Smart Electronics and Communication (ICOSEC), 2020.

3 Sreekanth K, Sreenivasappa & Veeranna B, *Design Parameters of Electric Vehicle,* International Conference on Power Electronics & IoT Applications in Renewable Energy and its Control (PARC), 2020.

4 Xue X D, Cheng K, & Cheung N.C, *Selection of Electric Motor Drives for electric vehicles*, Power Engineering Conference, 2008.

5 By Chunhua Liu. K.T., Chau, Christopher Lee. H.T., Zaixin Song. *A Critical Review of Advanced Electric Machines and Control Strategies for Electric Vehicles*, Proceedings of the IEEE, 109 (2021), 1004-1028.

6 Rahul Charles. C.M. & Savier. J.S, *Bidirectional DC-DC Converter Fed BLDC Motor in Electric Vehicle*, International Conference on Advances in Electrical, Computing, Communication and Sustainable Technologies (ICAECT), 2021.

7 Matthew Liam De Klerk & Akshay Kumar Saha, *Heliyon*, 8(2022).

8 Sheshadri Shekhar Rauth & Banshidhari Samanta, *Comparative Analysis of IM/BLDC/PMSM Drives for Electric Vehicle Traction Applications Using ANN-Based FOC*. IEEE 17th India Council International Conference (INDICON), 2020.

9 Rohullah Rahmatullah, Ayca. A.K. & Necibe Fusun Oyman Serteller, *Transportation Research Procedia, Elsevier*, 70 (2023),226-233.

10 Ristiana *et al*. R, *Advance BLDC Motor Drive Control for Electric Vehicles*, 8th International Conference on Wireless and Telematics (ICWT), Yogyakarta, Indonesia, 2023.

11 W Li,Xu Z, Zhang Y*, Induction motor control system based on FOC algorithm* at IEEE 8th Joint International Information Technology and Artificial Intelligence Conference (ITAIC), Chongqing, China, 2019.

12 Gora R, Biswas R, Garg. R K & Nangia U, *Field Oriented Control of Permanent Magnet Synchronous Motor (PMSM) Driven Electric Vehicle and Its Performance Analysis* at IEEE 4th International Conference on Computing, Power and Communication Technologies (GUCON), Kuala Lumpur, Malaysia. 2021.

13 Wei Liu, Tobias Placke & Chau. K.T, *Elsevier,* 4 (2022), 4058-4084.

14 Aditya & Mehdi Ferdowsi, *Comparison of NiMH and Li-ion Batteries in Automotive Applications* at IEEE Vehicle Power and Propulsion Conference (VPPC), 2008.

15 Hannana M A, Lipub M S H, Hussainb A & Mohamedb A, *Elsevier,* 78 (2017) 834.